IEEE Photonics Journal
An IEEE Photonics Society Publication

Open Access

PAPR Reduction in DCO-OFDM Visible Light Communication Systems Using Optimized Odd and Even Sequences Combination

Volume 11, Number 1, February 2019

Wei-Wen Hu, ***Member, IEEE***

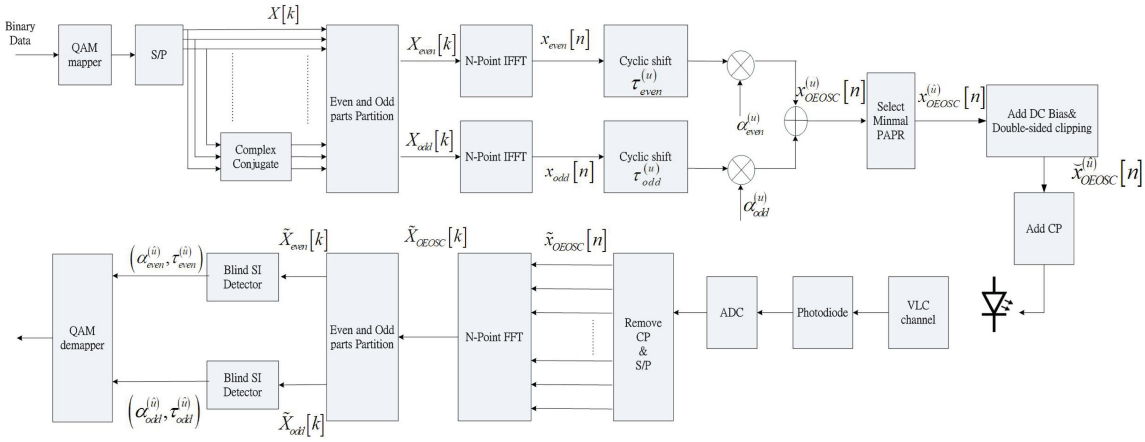

DOI: 10.1109/JPHOT.2019.2892871
1943-0655 © 2019 IEEE

PAPR Reduction in DCO-OFDM Visible Light Communication Systems Using Optimized Odd and Even Sequences Combination

Wei-Wen Hu, ***Member, IEEE***

Department of Electronic Engineering, Southern Taiwan University of Science and Technology, Tainan 71005, Taiwan

DOI:10.1109/JPHOT.2019.2892871

Manuscript received December 23, 2018; accepted January 9, 2019. Date of publication January 14, 2019; date of current version February 7, 2019. This work was supported by the Ministry of Science and Technology, R.O.C., under Grants MOST 107-2221-E-218-007-MY2 and MOST 107-2632-E-218-001.

Abstract: This paper proposes a novel peak-to-average power ratio (PAPR) reduction scheme, which has several advantages, such as low-complexity candidate construction and no side information (SI) transmission in direct current-biased optical orthogonal frequency division multiplexing (DCO-OFDM) visible light communication (VLC) systems. In the proposed scheme, the candidates can be generated by linearly combining time-domain even and odd sequences with cyclic shift and phase rotation. Even and odd sequences are obtained by adopting an inverse fast Fourier transform on the even and odd parts of a Hermitian symmetry encoded signal, respectively. Furthermore, a deterministic and efficient selection method of cyclic shift and phase rotation is derived to improve PAPR reduction performance and ensure that each candidate is unique, so that the receiver can recover the transmitted candidate signal without the use of SI. Simulation results show that the proposed scheme can achieve comparable PAPR reduction performance with the conventional selected mapping (CSLM) scheme with random and chaotic sequences, but at a considerably low computational complexity. Moreover, the proposed blind SI detection scheme provides almost the same bit error rate (BER) performance as that of the CSLM scheme with a perfect SI detection and symmetric selected mapping for a DCO-OFDM VLC system with 1024 subcarriers and 16-QAM. In contrast to other related time-domain sequences that combine methods used for DCO-OFDM systems, the proposed scheme improves BER performance with a slight increase in computational complexity and PAPR.

Index Terms: DCO-OFDM, SLM, sequence combination, Peak-to-average power ratio (PAPR), visible light communication.

1. Introduction

Orthogonal frequency division multiplexing (OFDM)-based visible light communication (VLC) has become a promising technology due to its advantages, such as high data rate, no harm to health, license-free spectrum, and no electromagnetic interference [1]. To obtain a high bandwidth efficiency and low complexity in implementation, direct current (DC)-biased optical orthogonal frequency division multiplexing (DCO-OFDM) has been widely used in VLC systems. However, a high peak-to-average power ratio (PAPR), which leads to severe light-emitting diode (LED) nonlinear clipping distortion, has been a major problem for DCO-OFDM VLC systems [2].

To overcome this problem, different PAPR reduction schemes conceived for DCO-OFDM VLC systems have been developed. In [3], [4], tone injection was performed using semidefinite relaxation and branch-and-bound methods, which achieve a substantial PAPR reduction. In [5], a modified active constellation extension algorithm was proposed to reduce the volume of DCO-OFDM VLC systems instead of PAPR. However, these methods can reduce the PAPR at the cost of transmission power consumption and computational complexity. Recently, tone reservation (TR)-based PAPR reduction schemes for avoiding transmission power consumption were proposed to DCO-OFDM VLC systems [6], [7]. However, the computational complexity associated with the TR method is high in searching peak-canceling signals. The research in [8], [9] introduced clipping and nonlinear companding algorithm as a simple means of reducing PAPR at the expense of severe bit error rate (BER) performance. In addition, pilot-aided methods for VLC systems were proposed in [10], [11] to improve PAPR reduction performance with the pre-defined pilot sequences. However, bandwidth efficiency is decreased due to the introduction of pilot sequences. Recently, a novel real-valued interleaved single-carrier frequency-division multiplexing (I-SC-FDM) scheme was proposed for optical systems. The PAPR reduction performance of I-SC-FDM is 10 and 7.5 dB smaller than those of the OFDM with QPSK and 16-QAM at the cost of spectrum efficiency and the required symbol duration, respectively [12].

In radio frequency (RF)-OFDM systems, the most popular technique for reducing the PAPR is selected mapping (SLM), which can be seen as a distortionless scheme. To adopt the SLM concept in DCO-OFDM VLC systems, various studies have been conducted [13]–[15]. The method proposed in [13] is to combine chaos with the SLM technique to control the construction of phase rotation factors. By contrast, [14] investigated SLM performance by using five different families of phase sequences, namely, chaotic, Shapiro-Rudin, pseudo-random interferometry code, Walsh-Hadamard, and random sequences, which result in different levels of PAPR reduction. SLM methods require a side information (SI) to indicate the transmitted candidate signal, which decreases bandwidth efficiency. The scheme in [15] adopted a special set of symmetric vectors as phase sequences to reduce the PAPR of DCO-OFDM VLC signals. Moreover, the magnitude difference between the received signal and pre-defined phase sequences in the frequency domain was used to detect the SI blindly. However, these methods have high computational complexity because they require multiple inverse fast Fourier transform (IFFT) operations to construct candidates. Although numerous low-complexity PAPR reduction schemes have been developed, they may not be suitable for VLC systems because the VLC signal is real and positive [16]–[21]. Two similar methods, namely, low-complexity selected mapping (LCSLM) [19] and cyclic selected mapping (CYSLM) [21], were developed for RF-OFDM systems, but both schemes suffer problems, for instance, the resultant frequency-domain phase sequences of the LCSLM and CYSLM schemes have an unequal magnitude, thereby causing degradation in BER performance. To the best of our knowledge, high computational complexity and SI transmission are still major issues in the design of PAPR reduction schemes for VLC systems.

In this paper, a novel PAPR reduction scheme using optimized even and odd sequence combination (OEOSC) technique is proposed for DCO-OFDM VLC systems to avoid SI transmission and a high computational complexity while maintaining the PAPR reduction capability. In the proposed OEOSC scheme, the candidates are produced by applying the linear combinations of the time-domain even and odd sequences with cyclic delay and phase shift. Th even and odd sequences are obtained by adopting IFFT on the even and odd parts of the Hermitian symmetry encoded signal, respectively. Moreover, we introduce the variance of correlation (VC) as a criterion for selecting the optimal cyclic shift and phase rotation values, thereby resulting in enhanced PAPR reduction performance and unique candidates. At the receiver, the natural diversity of cyclic shift and phase rotation for different candidates can be used to detect the SI blindly in the OEOSC scheme.

The main contributions of the OEOSC scheme used for DCO-OFDM VLC systems are as follows. First, the PAPR reduction performance of the OEOSC scheme using 32 candidate signals is worse than those of conventional selected mapping (CSLM) and symmetric selected mapping (SSLM) only by approximately 0.4 dB. However, the computational complexity of the OEOSC scheme is considerably lower than those of the CSLM and SSLM schemes. Second, in contrast to the LCSLM

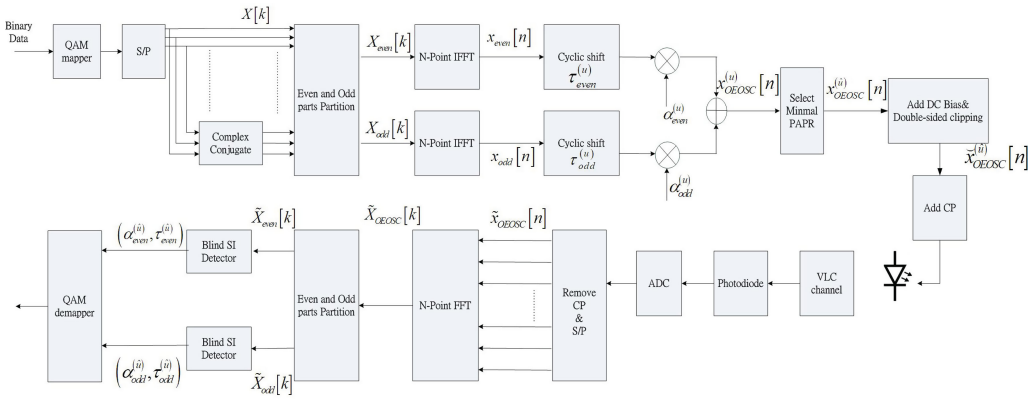

Fig. 1. The system block of the DCO-OFDM VLC transceiver with the proposed scheme.

and CYSLM schemes, the OEOSC scheme obtains improved BER performance because of the equal magnitude of the corresponding frequency domain phase sequences. Third, the proposed SI detection achieves almost the same BER performance as the CSLM scheme with perfect SI detection and the SSLM scheme.

The remainder of this paper is organized as follows. Section 2 introduces the DCO-OFDM VLC system model with the OEOSC scheme. The selection methods for candidate signals with SI blind detection and the improved PAPR reduction capability are also developed. Section 3 compares the computational complexity of the proposed OEOSC scheme with those of other existing PAPR reduction methods. Section 4 presents and discusses the simulation results for PAPR and BER performance. Finally, Section 5 provides brief concluding remarks.

2. OEOSC Scheme and SI Detector

2.1 OEOSC Scheme

Fig. 1 shows the system block of the DCO-OFDM VLC transceiver with the proposed OEOSC scheme and the corresponding SI detector. First, input binary data are modulated through M-ary quadrature amplitude modulation (M-QAM) from constellation ζ. To guarantee a real-valued VLC signal, the frequency-domain symbols to the IFFT block are constrained to have Hermitian symmetry:

$$X[N-k] = \bar{X}[k], \quad k = 0, 1, ..., N/2-1, \tag{1}$$

where N is the number of subcarriers and $\bar{X}$ denotes the complex conjugate of X. Data symbol $X[k]$ presents the modulated symbol with zero-mean and variance $E_X = E\left[|X[k]|^2\right]$, where $E[\cdot]$ refers to the expected value operation. Generally, the 0th and $\frac{N}{2}$th subcarriers are not loaded to avoid any residual complex components, i.e., $X[0] = X[N/2] = 0$. In the OEOSC scheme, the input data symbols after Hermitian symmetry encoding are decomposed into even and odd parts. For simplicity, we denote these parts of the Hermitian encoded symbol as X_{even} and X_{odd}, respectively, where the kth element of X_{even} and X_{odd} can be written as

$$X_{odd}[k] = \begin{cases} X[k], & k = 1, 3, \ldots, N/2-1 \\ \bar{X}[N-k], & k = N/2+1, \ldots, N-1 \\ 0, & \text{otherwise}, \end{cases} \tag{2}$$

$$X_{even}[k] = \begin{cases} X[k], & k = 0, 2, \ldots, N/2-2 \\ \bar{X}[N-k], & k = N/2+2, \ldots, N-2 \\ 0, & \text{otherwise}, \end{cases} \tag{3}$$

Then, frequency-domain sequences X_{even} and X_{odd} are transformed into two time-domain sequences, namely, $\mathbf{x}_{even} = \{x_{even}[n]\}_{n=0}^{N-1}$ and $\mathbf{x}_{odd} = \{x_{odd}[n]\}_{n=0}^{N-1}$, respectively, which can be written as

$$x_{odd}[n] = \frac{1}{\sqrt{N}} \sum_{\substack{k=0 \\ k\in odd}}^{N-1} X_{odd}[k] e^{j2\pi kn/N} = \frac{2}{\sqrt{N}} \sum_{\substack{k=1 \\ k\in odd}}^{N/2-1} \mathrm{Re}\{X[k] e^{j2\pi kn/N}\}, \tag{4}$$

$$x_{even}[n] = \frac{1}{\sqrt{N}} \sum_{\substack{k=0 \\ k\in even}}^{N-1} X_{even}[k] e^{j2\pi kn/N} = \frac{2}{\sqrt{N}} \sum_{\substack{k=1 \\ k\in even}}^{N/2-1} \mathrm{Re}\{X[k] e^{j2\pi kn/N}\}, \tag{5}$$

where $\mathrm{Re}\{\cdot\}$ is the real part of a complex value. $\mathbf{x}_{even}$ and $\mathbf{x}_{odd}$ are real-valued because frequency-domain sequences have the same Hermitian symmetry form as that of (1). Moreover, odd sequence $\mathbf{x}_{odd}$ has an anti-symmetric property in the time domain, whereas even sequence $\mathbf{x}_{even}$ has a periodical property as follows:

$$x_{odd}\left[n + \frac{N}{2}\right] = -x_{odd}[n], \ \ n = 0, 1, ..., N/2 - 1, \tag{6}$$

$$x_{even}\left[n + \frac{N}{2}\right] = x_{even}[n], \ \ n = 0, 1, ..., N/2 - 1 \tag{7}$$

Each time-domain sequence is independently cyclic-shifted and then multiplied with a phase rotation. Then, the uth candidate sequence $\mathbf{x}_{OEOSC}^{(u)} = \{x_{OEOSC}^{(u)}[n]\}_{n=0}^{N-1}$ can be generated by performing the linear combinations of the resulting time-domain sequences, given by

$$x_{OEOSC}^{(u)}[n] = \alpha_{odd}^{(u)} x_{odd}\left[(n - \tau_{odd}^{(u)})_N\right] + \alpha_{even}^{(u)} x_{even}\left[(n - \tau_{even}^{(u)})_N\right] \tag{8}$$

where $\alpha_{odd}^{(u)} \in \{\pm 1\}$, $\alpha_{even}^{(u)} \in \{\pm 1\}$, $\tau_{odd}^{(u)} \in \{0, 1, \ldots, N-1\}$, and $\tau_{even}^{(u)} \in \{0, 1, \ldots, N-1\}$. $(\cdot)_N$ denotes the modulo N operation defined as $(a)_N = a - \lfloor a/N \rfloor \times N$, indicating that the result of the modulo N operation in the proposed OEOSC scheme ranges from 0 to $N-1$ rather than from $-N/2$ to $N/2$. The PAPR of the uth transmitted signal $\mathbf{x}_{OEOSC}^{(u)}$ in the electrical domain is defined as

$$\mathrm{PAPR}(\mathbf{x}_{OEOSC}^{(u)}) = \frac{\max\limits_{0\le n\le N-1} |x_{OEOSC}^{(u)}[n]|^2}{E\left[|x_{OEOSC}^{(u)}[n]|^2\right]} \tag{9}$$

where the numerator is the maximum instantaneous power and the denominator represents the relating average power. In the OEOSC scheme, the candidate sequence with the minimum PAPR among U different candidates is selected for transmission, where the corresponding SI $\hat{u}$ is defined as

$$\hat{u} = \arg\min_{u=0,1,\ldots,U-1} \left(\mathrm{PAPR}(\mathbf{x}_{OEOSC}^{(u)})\right). \tag{10}$$

The selected real-valued bipolar signal $x_{OEOSC}^{(\hat{u})}[n]$ is then converted from parallel to serial. DC bias B_{DC} is added to the bipolar signal $x_{OEOSC}^{(\hat{u})}[n]$ to ensure that the transmitted signal is unipolar. B_{DC} is denoted as $B_{DC} = k\sqrt{E[|x_{OEOSC}^{(\hat{u})}[n]|^2]}$, where k indicates the clipping factor to avoid an excessive B_{DC} and minimize the transmitted optical power. In literature [2], this parameter is defined as a bias of $10 \cdot \log_{10}(k^2 + 1)$ dB. Then, to fit the linear transfer characteristic of the LED and improve the power efficiency, the biased signals are clipped at upper clipping level δ and at zero to obtain the

double-sided clipped signals as follows

$$\check{x}_{OEOSC}^{(\hat{u})}[n] = \begin{cases} \delta, & x_{OEOSC}^{(\hat{u})}[n] + B_{DC} \geq \delta, \\ x_{OEOSC}^{(\hat{u})}[n] + B_{DC}, & 0 < x_{OEOSC}^{(\hat{u})}[n] + B_{DC} < \delta, \\ 0, & x_{OEOSC}^{(\hat{u})}[n] + B_{DC} \leq 0, \end{cases} \tag{11}$$

When the forward voltage of biased signal $x_{OEOSC}^{(\hat{u})}[n] + B_{DC}$ is above δ or below zero, the nonlinear clipping distortion of the signal occurs. Then, the resulting real-valued positive signal adopted to drive the LED is represented as

$$\check{x}_{LED}[n] = x_{OEOSC}^{(\hat{u})}[n] + B_{DC} + n(B_{DC}), \tag{12}$$

where $n(B_{DC})$ enotes the noise component from the clipping operation. A cyclic prefix is then added to each real-valued positive clipped signal to avoid inter-symbol interference in optical multipath channels. At the receiver, the photodiode transfers the received optical signals to the electrical signals. After removing the DC bias and CP, the received frequency domain sequences with double-sided clipping degradation can be obtained by using N-point fast Fourier transform (FFT) operation as

$$\tilde{X}_{OEOSC}[k] = \frac{1}{\sqrt{N}} \sum_{k=0}^{N-1} \tilde{x}_{OEOSC}[n] e^{-j2\pi kn/N} = \tilde{X}_{OEOSC}^{(u)}[k]\tilde{H}[k] + \tilde{C}[k] + \tilde{W}[k], \tag{13}$$

where $\tilde{H}[k]$ and $\tilde{W}[k]$ represent the channel frequency response and AWGN noise at the kth sub-carrier, respectively, respectively. Clipping noise $\tilde{C}[k]$ in (13) is inversely proportional to the DC bias. Most of the CSLM-based PAPR reduction schemes can recover the transmitted signal by sending the SI through the dedicated channel and assuming a perfect SI detection at the receiver. To avoid the loss of bandwidth efficiency, we design a novel SI detector that recovers the transmitted signal in the following subsection.

2.2 Blind SI Detector

On the basis of Eq. (8), the OEOSC scheme can generate up to $4N^2$ alternative candidates by selecting cyclic shift and phase rotation of time-domain odd and even sequences. However, all $4N^2$ candidates are not unique and may not improve PAPR reduction performance. Generally, a set of U candidates from $4N^2$ candidates is required in practice. Thus, we should construct U candidates to improve PAPR reduction performance and ensure a correct recovery of U candidates at the receiver without the use of SI in the proposed OEOSC scheme. First, the criteria for constructing different candidates are investigated to enable the receiver to detect the transmitted signal blindly in this subsection. Selection criteria based on the correlation analysis of alternative candidates for improving PAPR reduction performance will be derived in the following subsection.

The uth candidate sequence $\mathbf{x}_{OEOSC}^{(u)}$ can be generated using (8). By considering the FFT of both sides of (8) and using the linear property of FFT, the kth element of the uth frequency-domain candidate sequence can be given by

$$X_{OEOSC}^{(u)}[k] = \alpha_{odd}^{(u)} X_{odd}[k] e^{j2\pi k\tau_{odd}^{(u)}/N} + \alpha_{even}^{(u)} X_{even}[k] e^{j2\pi k\tau_{even}^{(u)}/N} \tag{14}$$

On the basis of Eqs. (2) and (3), $X_{OEOSC}^{(u)}[k]$ is a combination of $X_{odd}[k]$ and $X_{even}[k]$, where the nonzero elements of $X_{odd}[k]$ and $X_{even}[k]$ are located at odd and even indices, respectively. As a result, $X_{odd}[k]$ and $X_{even}[k]$ do not overlap, thereby simplifying (14) as

$$X_{OEOSC}^{(u)}[k] = X[k] S_{OEOSC}^{(u)}[k] \tag{15}$$

where $S_{OEOSC}^{(u)}[k]$ is given by

$$S_{OEOSC}^{(u)}[k] = \begin{cases} \alpha_{odd}^{(u)} e^{j2\pi k \tau_{odd}^{(u)}/N}, & k \in \text{odd indices} \\ \alpha_{even}^{(u)} e^{j2\pi k \tau_{even}^{(u)}/N}, & k \in \text{even indices}, \end{cases} \tag{16}$$

The OEOSC can be regarded as an SLM scheme with phase sequence $S_{OEOSC}^{(u)}[k]$. A primary difference between the OEOSC and SLM-based schemes is that the phase sequence of the OEOSC scheme is polyphase, whereas that of the SLM-based scheme is quadriphase. Although the cyclic shift and phase rotation can be implemented in the frequency domain as shown in (14), they cannot help reduce the computational complexities. Hence, the cyclic shift and phase rotation of the proposed OEOSC scheme are implemented in the time domain.

To detect the selected candidate sequence blindly, each candidate sequence in the OEOSC scheme must be unique, that is, $X_{OEOSC}^{(u)}[k] \neq X_{OEOSC}^{(v)}[k]$ for $u \neq v$. In other words, the cyclic shift and phase rotation between the uth and vth candidate sequences must satisfy the following conditions to obtain $S_{OEOSC}^{(u)}[k] \neq S_{OEOSC}^{(v)}[k]$:

$$\alpha_{odd}^{(u)} e^{j2\pi k \tau_{odd}^{(u)}/N} - \alpha_{odd}^{(v)} e^{j2\pi k \tau_{odd}^{(v)}/N} \neq 0 \; k \in \text{odd indices}, \tag{17}$$

$$\alpha_{even}^{(u)} e^{j2\pi k \tau_{even}^{(u)}/N} - \alpha_{even}^{(v)} e^{j2\pi k \tau_{even}^{(v)}/N} \neq 0 \; k \in \text{even indices}, \tag{18}$$

We denote $\boldsymbol{\alpha}^{(u)} = [\alpha_{odd}^{(u)}, \alpha_{even}^{(u)}]$ and $\boldsymbol{\tau}^{(u)} = [\tau_{odd}^{(u)}, \tau_{even}^{(u)}]$ as the phase rotation and cyclic shift of the uth candidate sequence, respectively. Similarly, the phase rotation and cyclic shift of the vth candidate sequence is represented as $\boldsymbol{\alpha}^{(v)} = [\alpha_{odd}^{(v)}, \alpha_{even}^{(v)}]$ and $\boldsymbol{\tau}^{(v)} = [\tau_{odd}^{(v)}, \tau_{even}^{(v)}]$. According to (17) and (18), the conditions for constructing two different candidate sequences are derived in the following propositions.

Proposition 1: Given that the uth and vth candidate sequences are constructed from (8) with parameters $\boldsymbol{\alpha}^{(u)}$ and $\boldsymbol{\tau}^{(u)}$ and $\boldsymbol{\alpha}^{(v)}$ and $\boldsymbol{\tau}^{(v)}$,respectively, the uth candidate sequence is different from vth candidate sequence if $\boldsymbol{\alpha}^{(u)} = \boldsymbol{\alpha}^{(v)}$, $|\tau_{even}^{(v)} - \tau_{even}^{(u)}| \neq N/2$, and $|\tau_{odd}^{(v)} - \tau_{odd}^{(u)}| \neq 0$.

Proof: $\boldsymbol{\alpha}^{(u)} = \boldsymbol{\alpha}^{(v)}$ means that $\alpha_{odd}^{(u)} = \alpha_{odd}^{(v)}$ and $\alpha_{even}^{(u)} = \alpha_{even}^{(v)}$. Suppose that $\tau_{even}^{(v)} \neq \tau_{even}^{(u)} + N/2$ and $\tau_{odd}^{(v)} \neq \tau_{odd}^{(u)}$. Then, substituting $\alpha_{odd}^{(u)} = \alpha_{odd}^{(v)}$ and $\tau_{odd}^{(v)} \neq \tau_{odd}^{(u)}$ into (17), $\alpha_{odd}^{(u)}(e^{j2\pi k \tau_{odd}^{(u)}/N} - e^{j2\pi k \tau_{odd}^{(v)}/N}) \neq 0$. Substituting $\alpha_{even}^{(u)} = \alpha_{even}^{(v)}$ and $\tau_{even}^{(v)} \neq \tau_{even}^{(u)} + N/2$ into (18), $\alpha_{even}^{(u)}(e^{j2\pi k \tau_{even}^{(u)}/N} - e^{j2\pi k \tau_{even}^{(v)}/N}) \neq 0$. This concludes the proof of proposition 1. ■

Proposition 2: Given that the uth and vth candidate sequences are constructed from (8) with parameters $\boldsymbol{\alpha}^{(u)}$ and $\boldsymbol{\tau}^{(u)}$ and $\boldsymbol{\alpha}^{(v)}$ and $\boldsymbol{\tau}^{(v)}$,respectively, the uth candidate sequence is different from vth candidate sequence, the uth candidate sequence is different from vth candidate sequence if $\alpha_{odd}^{(u)} = \alpha_{odd}^{(v)}$, $\alpha_{even}^{(u)} = -\alpha_{even}^{(v)} |\tau_{even}^{(v)} - \tau_{even}^{(u)}| \neq 0$ or $N/2$, and $|\tau_{odd}^{(v)} - \tau_{odd}^{(u)}| \neq N/2$.

Proof: Suppose that $\alpha_{odd}^{(u)} = \alpha_{odd}^{(v)}$, $\alpha_{even}^{(u)} = -\alpha_{even}^{(v)}$, $\tau_{even}^{(v)} \neq \tau_{even}^{(u)} + N/2$ and $\tau_{odd}^{(v)} \neq \tau_{odd}^{(u)} + N/2$. Then, substituting $\alpha_{odd}^{(u)} = \alpha_{odd}^{(v)}$ and $\tau_{odd}^{(v)} \neq \tau_{odd}^{(u)} + N/2$ into (17), $\alpha_{odd}^{(u)}(e^{j2\pi k \tau_{odd}^{(u)}/N} - e^{j2\pi k \tau_{odd}^{(v)}/N}) \neq 0$. Substituting $\alpha_{even}^{(u)} = -\alpha_{even}^{(v)}$ and $\tau_{even}^{(v)} \neq \tau_{even}^{(u)}$ into (18), $\alpha_{even}^{(u)}(e^{j2\pi k \tau_{even}^{(u)}/N} - e^{j2\pi k \tau_{even}^{(v)}/N}) \neq 0$. This concludes the proof of proposition 2. ■

Proposition 3: Given that the uth and vth candidate sequences are constructed from (8) with parameters $\boldsymbol{\alpha}^{(u)}$ and $\boldsymbol{\tau}^{(u)}$ and $\boldsymbol{\alpha}^{(v)}$ and $\boldsymbol{\tau}^{(v)}$,respectively, the uth candidate sequence is different from vth candidate sequence, the uth candidate sequence is different from vth candidate sequence if $\alpha_{odd}^{(u)} = -\alpha_{odd}^{(v)}$, $\alpha_{even}^{(u)} = \alpha_{even}^{(v)} |\tau_{even}^{(v)} - \tau_{even}^{(u)}| \neq 0$ or $N/2$, and $|\tau_{odd}^{(v)} - \tau_{odd}^{(u)}| \neq N/2$.

Proof: The proof of Proposition 3 is similar to that of Proposition 2 and is omitted for brevity. ■

Propositions 1 and 2 allow the OEOSC scheme to select different candidate sequences, wherein the receiver can verify which candidate was transmitted without the use of SI. In practical systems, only the U candidate sequences are required for construction. When U distinct candidate sequences

are generated, the indices associated with the selected candidate sequence can be detected by

$$(\alpha_{odd}^{(\hat{u})}, \tau_{odd}^{(\hat{u})}) = \min_{\alpha_{odd}^{(u)}, \tau_{odd}^{(u)} \in \Omega} \sum_{k \in odd} \min_{X_{odd}[k] \in \zeta} \left| \tilde{X}_{odd}[k] e^{-j2\pi k \tau_{odd}^{(u)}/N} - X_{odd}[k] \alpha_{odd}^{(u)} \hat{H}_{odd}[k] \right|^2 \tag{19}$$

$$(\alpha_{even}^{(\hat{u})}, \tau_{even}^{(\hat{u})}) = \min_{\alpha_{even}^{(u)}, \tau_{even}^{(u)} \in \Omega} \sum_{k \in even} \min_{X_{even}[k] \in \zeta} \left| \tilde{X}_{even}[k] e^{-j2\pi k \tau_{even}^{(u)}/N} - X_{even}[k] \alpha_{odd}^{(v)} \hat{H}_{even}[k] \right|^2 \tag{20}$$

where $\Omega = \{\boldsymbol{\alpha}^{(u)}, \boldsymbol{\tau}^{(u)}, 0 \le u \le U-1\}$ is the set of U cyclic shift and phase rotation indices, which satisfies one proposition. $\hat{H}_{odd}[k]$ and $\hat{H}_{even}[k]$ refer to the estimated channel responses for odd and even subcarriers, respectively.

2.3 Correlation Analysis of Alternative Candidate Sequences

As mentioned in the previous subsection, the OEOSC scheme can construct a set of U different candidate sequences, which allows SI recovery associated with the selected candidate sequence blindly based on propositions 1, 2, and 3. However, the PAPR reduction capability should also be improved with the same set. In this subsection, a deterministic selection criterion for selecting cyclic shift and phase rotation is developed on the basis of the correlation analysis among alternative candidate sequences. The correlation between the uth and vth candidate sequences is expressed as

$$\begin{aligned} R_{uv}[m,n] &= E\left[x_{OEOSC}^{(u)}[m] \cdot \bar{x}_{OEOSC}^{(v)}[n]\right] \\ &= \frac{1}{N} E\left[\sum_{k=0}^{N-1} X_{OEOSC}^{(u)}[k] e^{j2\pi km/N} \cdot \sum_{k=0}^{N-1} \bar{X}_{OEOSC}^{(v)}[k] e^{-j2\pi kn/N}\right] \\ &= \frac{1}{N} E\left[\sum_{k=0}^{N-1} \sum_{l=0}^{N-1} X[k] \bar{X}[l] S_{OEOSC}^{(u)}[k] \bar{S}_{OEOSC}^{(v)}[l] e^{j2\pi(mk-nl)/N}\right] \\ &= \frac{1}{N} \sum_{k=0}^{N-1} S_{OEOSC}^{(u)}[k] \bar{S}_{OEOSC}^{(v)}[k] e^{j2\pi k\lambda/N} \end{aligned} \tag{21}$$

where $\lambda = m - n$ and the last equal sign is generated from $E[X[k]\bar{X}[l]] = 1$ if $k = l$; otherwise $E[X[k]\bar{X}[l]] = 0$. By substituting (16), (21) can be further expressed as

$$\begin{aligned} R_{uv}[\lambda] &= \frac{1}{N} \sum_{\substack{k=0 \\ k \in odd}}^{N-1} S_{OEOSC}^{(u)}[k] \bar{S}_{OEOSC}^{(v)}[k] e^{j2\pi k\lambda/N} + \frac{1}{N} \sum_{\substack{k=0 \\ k \in even}}^{N-1} S_{OEOSC}^{(u)}[k] \bar{S}_{OEOSC}^{(v)}[k] e^{j2\pi k\lambda/N} \\ &= \frac{1}{N} \sum_{k'=0}^{N/2-1} S_{OEOSC}^{(u)}[2k'+1] \bar{S}_{OEOSC}^{(v)}[2k'+1] e^{j2\pi\lambda/N} e^{j2\pi k'\lambda/(N/2)} \\ &\quad + \frac{1}{N} \sum_{k'=0}^{N/2-1} S_{OEOSC}^{(u)}[2k'] \bar{S}_{OEOSC}^{(v)}[2k'] e^{j2\pi k'\lambda/(N/2)} \\ &= \frac{1}{N} \sum_{k'=0}^{N/2-1} \alpha_{odd}^{(u)} \alpha_{odd}^{(v)} e^{j2\pi(2k'+1)(\tau_{odd}^{(u)} - \tau_{odd}^{(v)})/N} e^{j2\pi\lambda/N} e^{j2\pi k'\lambda/(N/2)} \\ &\quad + \frac{1}{N} \sum_{k'=0}^{N/2-1} \alpha_{even}^{(u)} \alpha_{even}^{(v)} e^{j2\pi 2k'(\tau_{even}^{(u)} - \tau_{even}^{(v)})/N} e^{j2\pi k'\lambda/(N/2)} \\ &= R_{odd}[\lambda] + R_{even}[\lambda] \end{aligned} \tag{22}$$

The correlation between the uth and vth candidate signals is highly dependent on the addition of $R_{odd}[\lambda]$ and $R_{even}[\lambda]$. $R_{odd}[\lambda]$ and $R_{even}[\lambda]$ can be regarded as the $N/2$-point IFFT of the sequence $S^{(u)}_{OEOSC}[2k'+1]\,\bar{S}^{(v)}_{OEOSC}[2k'+1]$ and $S^{(u)}_{OEOSC}[2k']\,\bar{S}^{(v)}_{OEOSC}[2k']$, respectively. In principle, low $R_{uv}[\lambda]$ indicates that $X^{(u)}_{OEOSC}[k]$ and $X^{(v)}_{OEOSC}[k]$ are poorly correlated. In [23], the VC was used to evaluate the PAPR reduction capability of different candidate sequence sets in SLM-based OFDM systems. VC is expressed as

$$\mathrm{VC} = \frac{\sum_{0\le u,v\le U-1,u\ne v}\mathrm{Var}\left[|R_{uv}[\lambda]|^2\right]_{\lambda=0}^{N-1}}{C_2^U} \tag{23}$$

where C_2^U is the binomial coefficient and Var[·] denotes the variance. The CSLM is a pattern-specific algorithm for PAPR reduction, wherein the optimal candidate sequence with minimal PAPR may be different for each OFDM symbol. However, the optimal candidate sequence set in the proposed OEOSC scheme is obtained from the minimization of the VC (Eq. (23)). The VC only depends on $R_{odd}[\lambda]$ and $R_{even}[\lambda]$ rather than $\mathbf{x}_{even}$ and $\mathbf{x}_{odd}$. Thus, the optimal candidate sequence set is irrelevant to the data symbols. Hence, we can determine the optimal candidate sequence set with U candidate sequences prior to data transmission and then maintain each OFDM symbol. When (19), (20) and (23) are combined, the OEOSC method aims to find an optimal set of candidate sequences that yields the transmitted sequence with the lowest PAPR and detects the transmitted sequence without SI. Consequently, the U candidate sequences can be obtained as

$$\arg\min_{\Omega}\frac{\sum_{0\le u,v\le U-1,u\ne v}\mathrm{Var}\left[|R_{uv}[\lambda]|^2\right]_{\lambda=0}^{N-1}}{C_2^U} \tag{24}$$

where Ω is given by (19) and (20).

3. Analysis of Computational Complexity

In the CSLM-based transmitter, the computational complexity is often evaluated in terms of the required number of IFFT operations because the candidate signals are constructed in the frequency domain. However, calculating the additional operations in the time domain is necessary if the candidate signals are constructed in the time domain. Thus, the overall computational complexity for the CSLM, SSLM, LCSLM, CYSLM, and OEOSC schemes are analyzed by calculating the required number of real multiplications and additions because the VLC signal is real and positive. At the receiver, the computational complexity of the proposed blind SI detection is also compared with that of the ML detector in the SLM-based blind SI detection.

3.1 Computational Complexity for the Transmitter

In analyzing computational complexity for the transmitter, we exclude the minimization computational complexity for obtaining the signal with the lowest PAPR because the complexity is identical for all schemes. The number of candidate sequences is assumed to be U. The CSLM and SSLM schemes require U IFFT operations with U candidate sequences. Each N-point IFFT operation requires $(N/2)\log_2 N$ complex multiplications and $N\log_2 N$ complex additions. One complex multiplication involves four real multiplications and two real additions, whereas one complex addition involves two real additions. Therefore, the total numbers of real multiplications and additions required in the CSLM and SSLM schemes are $(2UN)\log_2 N$ and $(3UN)\log_2 N$, respectively. Additional $8US$ real multiplications are required by the SSLM scheme, where S is the number of subcarriers that must be amplified within the first quarter of subcarriers. Thus, the total real multiplications and additions for the SSLM scheme are $(2UN)\log_2 N + 8US$ and $3UN\log_2 N$, respectively.

TABLE 1
Computational Complexity Comparison of the CSLM, the LCSLM, CYSLM and the OEOSC Schemes

	Real Multiplications	Real Additions	Number of SI bits
CSLM [12]	$(2UN)\log_2 N$	$(3UN)\log_2 N$	$\log_2 U$
LCSLM [18]	$(4N)\log_2 N + N$	$(6N)\log_2 N + (U-2)N$	$\log_2 U$
CYSLM [20]	$(2N)\log_2 N$	$(3N)\log_2 N + (U-1)DN$	$\log_2 U$
SSLM [14]	$(2UN)\log_2 N + 8US$	$(3UN)\log_2 N$	0
OEOSC	$(4N)\log_2 N$	$(6N)\log_2 N + UN$	0

In the LCSLM scheme [19], the uth candidate sequence of LCSLM is given as

$$x^{(u)}_{\text{LCSLM}}[n] = \begin{cases} x^{(u)}_{\text{CSLM}}[n], & 0 \le u \le 1 \\ x^{(0)}_{\text{CSLM}}[n] + \alpha x^{(1)}_{\text{CSLM}}\left[(n - \tau^{(u)}_{\text{LCSLM}})_N\right], & 2 \le u \le U-1 \end{cases} \tag{25}$$

where $0 < \alpha \le 1$ is a linear factor and $\tau^{(u)}_{\text{LCSLM}} \in \{1, 2, \ldots, N-1\}$ denotes the amount of cyclic shift for the uth (i.e., $u \ge 2$) candidate sequence. On the basis of Eq. (25), the LCSLM requires two IFFT operations with two candidate sequences, namely, $x^{(0)}_{\text{CSLM}}[n]$ and $x^{(1)}_{\text{CSLM}}[n]$. Moreover, $(U-2)N$ real additions are required to construct extra $U-2$ new candidates as given by (25) and N real multiplications are required to compute $\alpha x^{(1)}_{\text{CSLM}}[(n - \tau^{(u)}_{\text{LCSLM}})_N]$. Finally, the total numbers of real multiplications and additions required for the LC-SLM scheme are $4N\log_2(N) + N$ and $6N\log_2(N) + (U-2)N$, respectively.

In the CYSLM scheme [21], the uth candidate signal is constructed by combining the original signal $x[n]$ with D cyclic shift equivalents under the phase shift, given by

$$x^{(u)}_{\text{CYSLM}}[n] = \begin{cases} x[n], & u = 0 \\ x[n] + \sum_{d=1}^{D} \alpha^{(u)}_d x\left[(n - \tau^{(u)}_{\text{CYSLM},d})_N\right], & 1 \le u \le U-1 \end{cases} \tag{26}$$

where $\alpha^{(u)}_d \in \{\pm 1\}$ and $\tau^{(u)}_{\text{CY-SLM},d} \in \{1, 2, \ldots, N-1\}$ denote the amount of cyclic shift for dth branch signal. As shown in (26), the CY-SLM scheme requires one IFFT operation to construct $x[n]$ and DN real additions to generate one candidate sequence when superposing $x[n]$ and D phase shifted cyclic delay signals. Finally, the generation of U candidate signals in (26) requires $2N\log2(N)$ real multiplications and $3N\log2(N) + (U-1)DN$ real additions.

In the proposed OEOSC scheme, two IFFT operations are required to construct $x_{odd}[n]$ and $x_{even}[n]$. Additional N real additions are required by the OEOSC scheme to combine $x_{odd}[n]$ and $x_{even}[n]$ to obtain one candidate sequence. Thus, the total numbers of real multiplications and additions for generating U candidate sequences are $4N\log2(N)$ and $6N\log 2(N) + UN$, respectively.

Table 1 summarizes the required number of the real multiplications, real additions, and SI bits of the five schemes. Fig. 2 shows the numerical results for the case of $N = 1024$ for a different number of candidate sequences. D was set to be two in the CYSLM scheme. The SSLM scheme has almost identical computational complexities to the CSLM scheme, but the SSLM does not require SI transmission. The OEOSC scheme achieves a considerably reduced complexity than the CSLM and SSLM schemes without BER degradation. In addition, the CYSLM scheme has the lowest computational complexity at the cost of BER degradation and data rate loss. Although the number of SI bits for the CSLM, LCSLM, and CYSLM is small when high-order modulation types are used, forward error coding is often required to prevent erroneous SI detection, which causes loss of data symbol. The introduction of forward error coding not only reduces the data rate but also renders the receiver further complex. As a result, the total redundancy may exceed $\log_2 U$

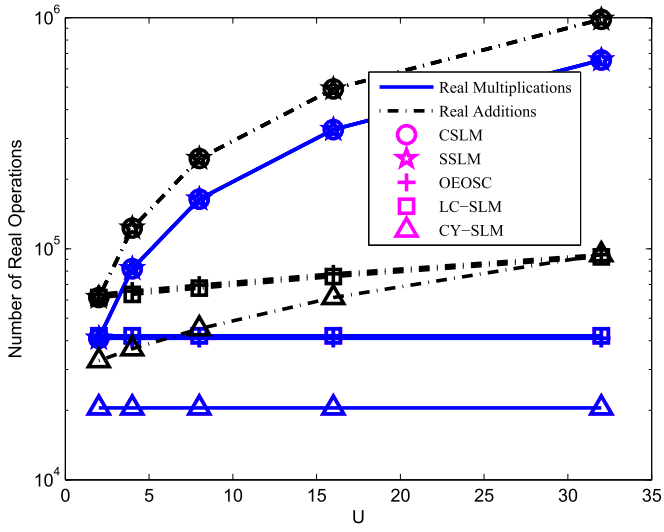

Fig. 2. Total number of real multiplications and real additions for different U values with $N = 1024$.

TABLE 2
Computational Complexity Comparison of Differnet SI Blind Detection Schemes

	Real Multiplications	Real Additions
ML [22]	$2UM^N$	UM^N
SSLM [15]	$8NU$	$5NU$
OEOSC	$4(1+2M)UN$	$2(1+3M)UN$

bits. Therefore, providing a quantitative analysis of the bandwidth efficiency is difficult because the bandwidth efficiency depends on the adopted forward error coding. To be fair with other SLM-based schemes, we only listed the number of SI bits in Table 1 without considering forward error coding.

3.2 Computational Complexity for the Receiver

The receiver computational complexity of the proposed OEOSC scheme is evaluated in this subsection. For each odd subcarrier, (19) shows that the blind SI detector requires two complex multiplications and one complex addition to calculate the squared absolute operation, wherein two complex multiplications are required for $\tilde{X}_{odd}[k]\, e^{-j2\pi k\tau_{odd}^{(u)}/N}$ and $X_{odd}[k]\,\alpha_{odd}^{(u)}\hat{H}_{odd}[k]$ and one complex addition is required for the addition of $\tilde{X}_{odd}[k]\, e^{-j2\pi k\tau_{odd}^{(u)}/N}$, $X_{odd}[k]\,\alpha_{odd}^{(u)}\hat{H}_{odd}[k]$. Then, one complex multiplication is also required for the squared absolute operation. Given the U candidate sequences, N subcarriers, and M-QAM constellation, the computational complexity of the proposed blind SI detection is approximately $(1+2M)UN/2$ complex multiplications and $UMN/2$ complex additions by omitting the operation of summation required in (19). On the basis of Eq. (20), the complexity is the same as that in an odd subcarrier. As one complex multiplication involves four real multiplications and two real additions and that one complex addition involves two real additions, the overall computational complexities of real multiplications and additions for the OEOSC scheme are calculated as $4(1+2M)UN$ and $2(1+3M)UN$, respectively. Table 2 presents the computational complexity of various blind SI detection schemes. Numerical analysis indicates that the computational complexity of the proposed SI detection is considerably lower than that of the SLM with ML detection. Although the computational complexity of the proposed SI detection is slightly larger than that of the SSLM, the relating transmitter has a considerably lower computational complexity, as shown in Table 1.

TABLE 3
System Parameters for Simulation

Number of subcarriers, N	1024
Length of cyclic prefix	$N/16 = 64$
Total number of OFDM symbols	10^6
Number of channel impulse response	10
Modulation scheme	16-QAM
QAM symbol energy, E_X	unity
B_{DC}	7 dB or 5 dB
$k = \sqrt{10^{(B_{DC}/10)} - 1}$	2, 1.47
δ	4, 2.94
τ	50 ns

4. Simulation Results

In this section, simulation results of the proposed OEOSC scheme for DCO-OFDM VLC systems are evaluated in terms of PAPR reduction and BER. For the purpose of comparison, the CSLM, SSLM, LCSLM, and CYSLM schemes and direct clipping are considered in the simulations. Following [24], the LED nonlinear model is regarded as the double-sided clipping in Eq. (11), where B_{DC} is set to $\delta/2$ to ensure a steady dynamic region. The simulated channel impulse response of the multipath optical channel is $h(t) = \frac{1}{\tau} exp(\frac{-t}{\tau})u(t)$, where $u(t)$ represents the unit step function and τ denotes the exponential decay time constant [25]. In our simulations, we use simple least squares to estimate the frequency-domain channel response in all methods. The PAPR reduction performance is evaluated using a complementary cumulative distribution function (CCDF), defined as the probability that the PAPR exceeds a given threshold γ as follows:

$$\text{CCDF}_{\text{PAPR}(\mathbf{x}^{(u)}_{OEOSC})}(\gamma) = \text{Prob}[\text{PAPR}(\mathbf{x}^{(u)}_{OEOSC}) > \gamma]. \tag{27}$$

Table 3 lists the system parameters applied in the simulation. The clipping ratio depends on the required DC bias level. In our simulations, we consider cases $B_{DC} = 5$ dB and $B_{DC} = 7$ dB, which lead to clipping levels of $\delta = 2.94$ and $\delta = 4$, respectively. Moreover, the noise source used in our simulation is AWGN noise.

4.1 Comparison With SLM-Based PAPR Reduction Scheme

In the proposed OEOSC scheme, the selection criterion of candidate signals is based on the minimization of the VC defined in Eq. (23). Different sequence sets have different VC values. Simulation results (figures omitted here for brevity) have shown that the improvement in the PAPR reduction performance of the CSLM and OEOSC schemes is small in the case of 1024 subcarriers and 16-QAM modulation when $U \geq 32$. To provide the best balance between computational complexity and PAPR reduction performance, a value of $U = 32$ is adopted in all PAPR reduction schemes For Figs. 3 and 4, the B_{DC} is set to 7 dB, which leads to $k = 2$ and $\delta = 4$. Thus, when the forward voltage of the biased signal is above four or below zero, the nonlinear clipping distortion of the signal occurs.

Fig. 3 demonstrates the CCDF of the proposed OEOSC scheme, of which each $\boldsymbol{\alpha}^{(u)}$ and $\boldsymbol{\tau}^{(u)}$ belong to Ω. In addition, we plot the CCDFs of the CSLM scheme with a set of Walsh-Hadamard, chaotic, and random sequences as phase sequences for comparison. We observe that the CSLM scheme with chaotic and random sequences has the best PAPR reduction performance because the VC values of the random and chaotic sequence sets are the lowest. Although the performance loss of the OEOSC scheme relative to that of the CSLM with these two sequence sets is found to be

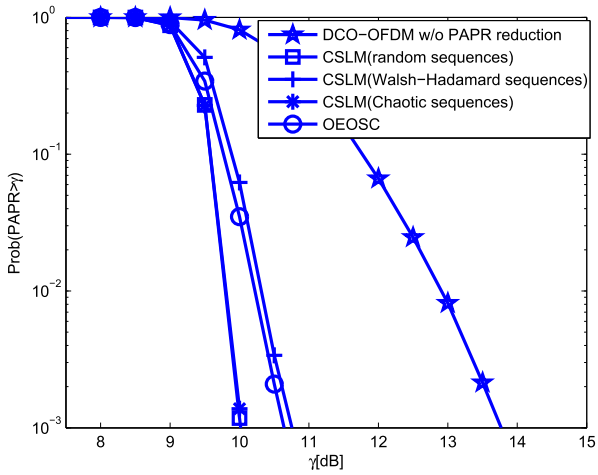

Fig. 3. Comparison of PAPR reduction performance of CSLM using different phase sequences sets($N = 1024$ and $U = 32$).

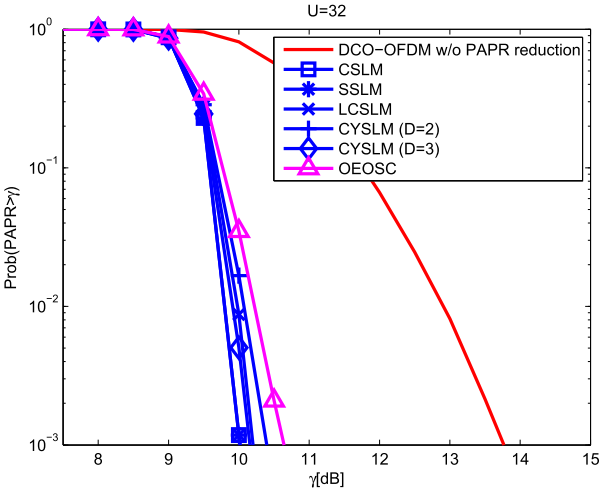

Fig. 4. Comparison of PAPR reduction performance for the original DCO-OFDM, direct clipping, CSLM, the LC-SLM, CY-SLM and the TDEOSC schemes($N = 1024$ and $U = 32$).

0.6 dB for $U = 32$ and Prob[PAPR($\mathbf{x}^{(u)}_{OEOSC}$) $> \gamma$] $= 10^{-3}$, the OEOSC scheme has the advantages of considerably low complexity and no SI transmission.

Fig. 4 displays the PAPR reduction performances of different PAPR reduction schemes in DCO-OFDM VLC systems. In simulating the performance of the CSLM scheme, the phase sequences are selected from random sequences. In the SSLM scheme, the best amplification factor for balancing the BER and PAPR reduction performances is 1.8 when we set $S = 1$; as a result, four subcarriers must be amplified. Moreover, the LCSLM and CYSLM schemes randomly select cyclic shifts $\tau^{(u)}_{\text{LC-CSLM}}$ and $\tau^{(u)}_{\text{CY-SLM},d}$ between 1 and $N - 1$. Fig. 4 shows that the PAPR reduction performance of the CSLM and SSLM schemes is exactly the same because the candidate sequences are constructed in the frequency domain for both schemes. The results in Fig. 4 also indicate that the PAPR reduction performance of the LCSLM and CYSLM methods is slightly worse than that of the CSLM and SSLM. This finding can be demonstrated by the fact that the candidate sequences of the LCSLM and CYSLM methods are constructed in the time domain. However, the computational complexities of the LCSLM and CYSLM methods are considerably lower than those of the CSLM and SSLM

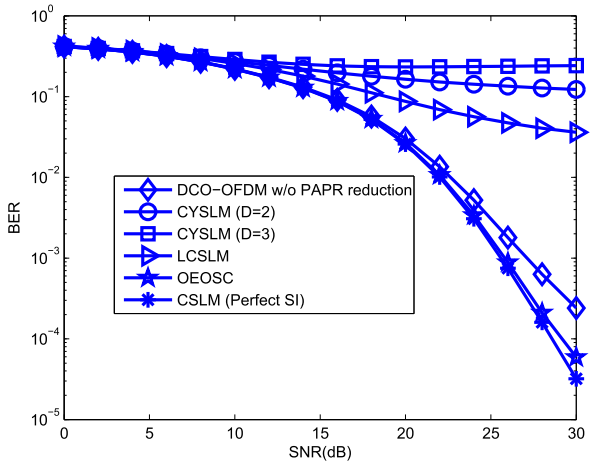

Fig. 5. Comparison of BER performance for DCO-OFDM systems with various PAPR reduction schemes ($B_{DC} = 7$ dB, $U = 32$).

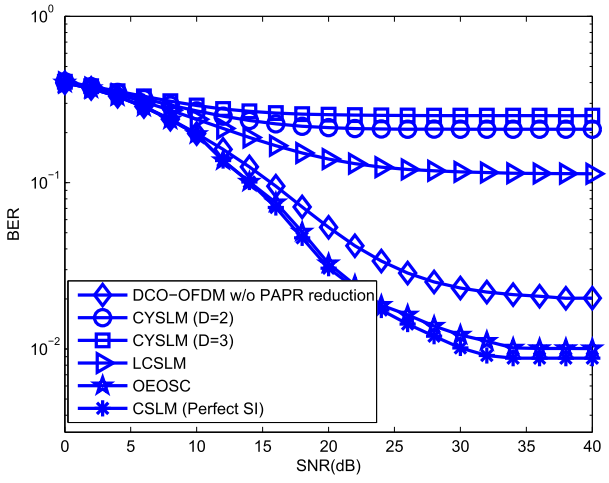

Fig. 6. Comparison of BER performance for DCO-OFDM systems with various PAPR reduction schemes ($B_{DC} = 5$ dB, $U = 32$).

schemes. The PAPR reduction performance of the proposed OEOSC scheme is slightly worse than that of the LC-SLM and CY-SLM methods by approximately 0.1 $\sim$ 0.2 dB for $U = 32$ and Prob[PAPR($\mathbf{x}^{(u)}_{OEOSC}$) $> \gamma$] $= 10^{-3}$. Nevertheless, the proposed scheme has better BER performance than the LCSLM and CYSLM because of the equal magnitude of the corresponding frequency-domain phase sequences, as demonstrated in the following simulation results.

Figs. 5 and 6 demonstrate the BER performance of different PAPR reduction methods in DCO-OFDM VLC systems given by $B_{DC} = 7$ dB and $B_{DC} = 5$ dB, respectively. The linear transfer characteristic of the LED as expressed by Eq. (11) is considered in both figures. The channel estimation must be known at the receiver end for all schemes by using the simple least square method. In Fig. 5, the proposed OEOSC scheme enjoys a remarkable BER performance improvement compared with the LCSLM and CYSLM schemes because of the equal magnitude of the corresponding frequency domain phase sequences. Moreover, the OEOSC scheme can provide almost the same BER performance as the CSLM scheme with perfect SI, but at a considerably low computational complexity. However, for a low DC bias level of 5 dB, the DCO-OFDM system without PAPR reduction yields a BER plateau due to the large clipping noise. The OEOSC scheme can reduce the level

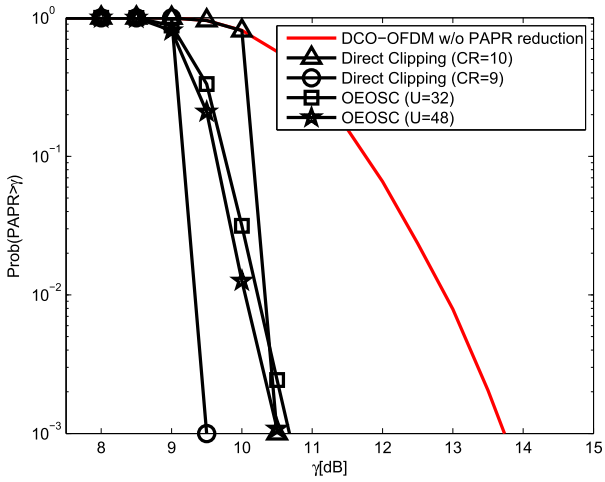

Fig. 7. CCDF performance of the OEOSC scheme and direct clipping scheme for 16-QAM($B_{DC} =$ 5 dB, $U = 32$).

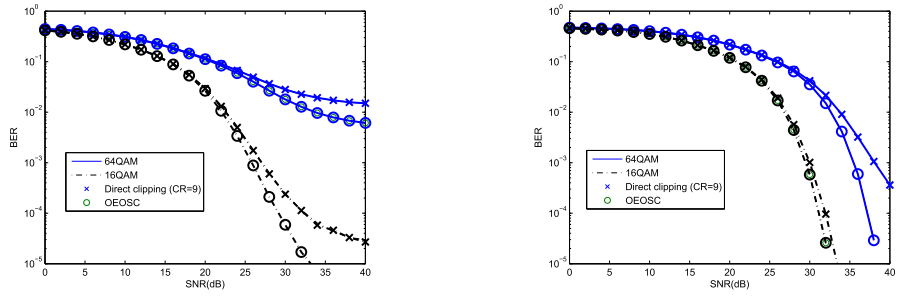

(a) (b)

Fig. 8. Comparison of BER performance of direct clipping and the OEOSC scheme for 16-QAM and 64-QAM modulation (a) $B_{DC} = 7$ dB, (b) $B_{DC} = 13$ dB.

of error floor because of its improved PAPR reduction capability. Therefore, the PAPR reduction scheme must be applied in DCO-OFDM VLC systems with a low DC bias level.

4.2 Comparison With Direct Clipping PAPR Reduction Scheme

In this subsection, we further present the simulation results that illustrate the performance comparison between the OEOSC and direct clipping schemes. The differences between these schemes are stated as follows. First, direct clipping requires further filtering to reduce the out-of-band emission, which may reintroduce additional peaks. On the contrary, the proposed OEOSC scheme does not increase out-of-band emission with respect to pure DCO-OFDM without PAPR reduction. Importantly, clipping and filtering also produce in-band distortions that degrade the BER, whereas the OEOSC scheme does not produce in-band distortions.

Fig. 7 shows that the maximum performance losses of the OEOSC scheme with 32 candidate signals relative to the direct clipping scheme with CR = 9 dB and CR = 10 dB are approximately 1.2 and 0.2 dB for the CCDF of 10^{-3} under 16-QAM modulation, respectively. However, the OEOSC scheme enjoys a remarkable BER performance improvement. For example, as shown in Fig. 8(a) and given a 7 dB BDC (i.e., low biasing level), the SNR improvement of the OEOSC scheme is 3.5 dB at a BER of 10^{-4} and 16-QAM modulation. Moreover, the proposed OEOSC scheme can reduce the error-free level for 64-QAM modulation. By contrast, given a 13 dB BDC (i.e., large biasing level) and at a BER of 10^{-4}, the proposed OEOSC scheme achieves 0.2 and 3 dB gains for 16-QAM and 64-QAM modulations, respectively.

5. Conclusions

A novel PAPR reduction scheme based on the OEOSC is proposed for DCO-OFDM VLC systems. Simulation results show that the OEOSC scheme has almost the same BER performance as the CSLM scheme, but the OEOSC scheme has a considerably lower computational complexity. In comparison with the existing LCSLM and CYSLM schemes, the OEOSC scheme has the advantage of improving the BER and PAPR reduction performances with only marginal computational complexity cost. This condition is due to the equal magnitude of the corresponding frequency domain phase sequences and the degree of freedom in selecting the cyclic shift values, respectively.

References

[1] O. Narmanlioglu, R. C. Kizilirmak, F. Miramirkhani, and M. Uysal, "Cooperative visible light communications with full-duplex relaying," *IEEE Photon. J.*, vol. 91, pp. 1–11, May 2017, Art. no. 7900111.

[2] J. Armstrong and B. Schmidt, "Comparison of asymmetrically clipped optical OFDM and DC-biased optical OFDM in AWGN," *IEEE Commun. Lett.*, vol. 12, no. 5, pp. 343–345, May 2008.

[3] H. Zhang, Y. Yuan, and W. Xu, "PAPR reduction for DCO-OFDM visible light communications via semi definite relaxation," *IEEE Photon. Technol. Lett.*, vol. 26, no. 17, pp. 1718–1721, Sep. 2014.

[4] Y. Hei, J. Liu, W. Li, X. Xu, and R. T. Chen, "Branch and bound methods based tone injection schemes for PAPR reduction of DCO-OFDM visible light communications," *Opt. Exp.*, vol. 25, no. 2, pp. 595–604, Jan. 2017.

[5] J. Garcia Doblado, A. Cinta Oria Oria, V. Baena-Lecuyer, and P. Lopez, "Cubic metric reduction for DCO-OFDM visible light communication systems," *J. Lightw. Technol.*, vol. 33, no. 10, pp. 1971–1978, May 2015.

[6] J. Bai, Y. Li, Y. Yi, W. Cheng, and H. Du, "PAPR reduction based on tone reservation scheme for DCO-OFDM indoor visible light communications," *Opt. Exp.*, vol. 25, no. 20, pp. 24630–24638, Oct. 2017.

[7] Y. Hei, J. Liu, H. Gu, W. Li, X. Xu, and R. T. Chen, "Improved TKM-TR methods for PAPR reduction of DCO-OFDM visible light communications," *Opt. Exp.*, vol. 25, no. 20, pp. 24448–24458, Oct. 2017.

[8] Z. Yu, R. J. Baxley, and G. T. Zhou, "Iterative clipping for PAPR reduction in visible light OFDM communications," in *Proc. IEEE Military Commun. Conf.*, May 2014, pp. 1681–1686.

[9] K. Bandara, P. Niroopan, and Y. H. Chung, "PAPR reduced OFDM visible light communication using exponential nonlinear companding," in *Proc. IEEE Int. Conf. Micro. Commun. Antenna Elect. Syst.*, Oct. 2013, pp. 1–5.

[10] W. O. Popoola, Z. Ghassemlooy, and B. G. Stewart, "Pilot-assisted PAPR reduction technique for optical OFDM communication systems," *J. Lightw. Technol.*, vol. 32, no. 7, pp. 1374–1382, Apr. 2014.

[11] F. B. Ogunkoya, W. O. Popoola, A. Shahrabi, and S. Sinanovic, "Performance evaluation of pilot-assisted PAPR reduction technique in optical OFDM systems," *IEEE Photon. Technol. Lett.*, vol. 27, no. 10, pp. 1088–1091, May 2015.

[12] J. Zhou *et al.*, "Interleaved single-carrier frequency-division multiplexing for optical interconnects," *Opt. Exp.*, vol. 25, no. 9, pp. 10586–10596, Apr. 2017.

[13] Y. Xiao, M. Chen, F. Li, T. Tang, Y. Liu, and L. Chen, "PAPR reduction based on chaos combined with SLM technique in optical OFDM IM/DD system," *Opt. Fiber Technol.*, vol. 21, pp. 81–86, Jan. 2015.

[14] M. Z. Farooqui, P. Saengudomler, S. Kaiser, "Average transmit power reduction in OFDM-based indoor wireless optical communications using SLM," in *Proc. 6th Int. Conf. Elect. Comput. Engine.*, Dec. 2010, pp. 602–605.

[15] W. W. Hu and D. H. Lee, "PAPR reduction for visible light communication systems without side information," *IEEE Photon. J.*, vol. 9, no. 3, Jun. 2017, Art. no. 7202411.

[16] C. L. Wang and Y. Ouyang, "Low-compplexity selected mapping scheme for peak-to-average power ratio reduction in OFDM systems," *IEEE Trans. Signal Process.*, vol. 53, no. 12, pp. 4652–4660, Dec. 2005.

[17] C. P. Li, S. H. Wang, and C. L. Wang, "Novel low-complexity SLM schemes for PAPR reduction in OFDM systems," *IEEE Trans. Signal Process.*, vol. 58, no. 5, pp. 2916–2921, May 2010.

[18] E. Alsusa and L. Yang, "A low-complexity time-domain linear symbol combining technique for PAPR reduction in OFDM systems," *IEEE Trans. Signal Process.*, vol. 56, no. 10, pp. 4844–4855, Oct. 2008.

[19] L. Yang, K. K. Soo, Y. M. Siu, and S. Q. Li, "A low complexity selected mapping scheme by use of time domain sequence superposition technique for PAPR reduction in OFDM system," *IEEE Trans. Broadcast.*, vol. 54, no. 4, pp. 821–824, Dec. 2008.

[20] S. S. Eom, H. Nam, and Y. C. Ko, "Low-complexity PAPR reduction scheme without side information for OFDM systems," *IEEE Trans. Signal Process.*, vol. 60, no. 7, pp. 3657–3669, Jul. 2012.

[21] P. D. Pamungkasari and Y. Sanada, "Time domain cyclic-selective mapping for PAPR reduction using delayed correlation with matched filter in OFDM system," in *Proc. IEEE Int. Conf. Telecommun.*, Apr. 2015, pp. 373–377.

[22] A .D. S. Jayalath and C. Tellambura, "SLM and PTS peak-power reduction of OFDM signals without side information," *IEEE Trans. Wireless Commun.*, vol. 4, no. 5, pp. 2006–2013, Sep. 2005.

[23] J. Y. Woo, H. S. Joo, K. H. Kim, J. S. No, and D. J. Shin, "PAPR analysis of class-III SLM scheme based on variance of correlation of alternative OFDM signal sequences," *IEEE Commun. Lett.*, vol. 19, no. 6, pp. 989–992, Jun. 2015.

[24] J. Tan, Z. Wang, Q. Wang, and L. Dai, "Near-optimal low-complexity sequence detection for clipped DCO-OFDM," *IEEE Photon. Technol. Lett.*, vol. 28, no. 3, pp. 233–236, Feb. 2016.

[25] J. Carruthers and J. Kahn, "Modeling of nondirected wireless infrared channels," *IEEE Trans. Commun.*, vol. 45, no. 10, pp. 1260–1268, May 1997.